THE ERROR ANALYSIS AND SENSITIVITY ANALYSIS OF CABLE-TYPING CLOSE-COUPLING MULTI-ROBOTS TOWING SYSTEM

Zhirui WANG [1], Zhigang ZHAO[2],Cheng SU[3], Kaiyi TANG[4]

Cable-typing close-coupling multi-robots towing system is a new kind of multi-robots parallel system. Firstly, the kinematics model of the whole system is established by using D-H method and homogeneous transfer matrix. D-H method uses homogeneous transfer matrix to describe the spatial relationship between two linkages. Based on the kinematics model, the system comprehensive error model is built by using the total differentiation method. The sensitivity of each error source in the whole system and the reliability of the motion accuracy of the system output are analyzed. The numerical simulation of an example is carried out with MATLAB. The research shows that the established system integrated error model, sensitivity model and motion accuracy reliability model can effectively reflect the influence of input error on the system output. It provides a theoretical basis for improving the motion accuracy of the parallel robots.

Keywords: multi-robot lifting; kinematics model; position error; sensitivity analysis; motion reliability

1. Introduction

Cable-typing close-coupling multi-robots towing system (CCMRTS) is a new structure with both multi-robot system and parallel robot characteristics. It has the advantages of simple structure, large workspace, easy disassembly and assembly, reconfiguration, high modularity, strong load capacity, fast moving speed and so on. In recent years, the application of CCMRTS has been increasing.

[1] Master, School of Mechatronic Engineering, Lanzhou Jiaotong University, Lanzhou, China，e-mail: 1192126871@qq.com

[2] Prof., School of Mechatronic Engineering, Lanzhou Jiaotong University, Lanzhou, China，e-mail: flapping@21cn.com

[3] Associate Prof., School of Mechatronic Engineering, Lanzhou Jiaotong University, Lanzhou, China，e-mail: sucheng@21cn.com

[4] Master, School of Mechatronic Engineering, Lanzhou Jiaotong University, Lanzhou, China，e-mail: 408939812@qq.com

Therefore, the research of it has important academic value and practical engineering application value[1].

Scholars at home and abroad have done a lot of theoretical research on cable parallel robots, and designed abundant configurations to be applied in different working situations. The research of cable parallel robots includes many complex aspects, such as kinematics and dynamics, trajectory planning, motion stability control, motion accuracy and reliability. Cable-typing close-coupling multi-robots towing system is a new multi-machine coordination system based on cable parallel robots, so it can be used for reference in the process of theoretical research.

Many scholars have conducted in-depth research on different configurations of CCMRTS, and have formed a certain theoretical system. Kumar[2-4] et al. established a 6-DOF coordinated lifting system through three aerial robots, established the statics equilibrium equation of system , and analyzed the kinematics, dynamics and stability of the system. Cheng Peng[5] et al. discussed the coordinated dragging of an object on the ground in a smooth flat room by using multiple ground mobile robots. Considering the constraints of dry friction and restraining tensile force, the differential equations of motion of the system were established, and the trimming conditions under different system configurations were discussed. Zheng Yaqing[6-7] et al. designed different lifting structures, but made the whole lifting system into a specific mechanism, which greatly limited the system's motion performance. Zi Bin[8-9] and others systematically researched about dynamics, static workspace and motion error of hybrid-driven based cable parallel robots. Zhao Zhigang[10-14] et al. designed the under-constraint multi-crane hoisting system, established a virtual simulation experimental platform by using several software, and built a solid experimental platform. The kinematics and dynamics equations of the system are established, and the stability control and trajectory planning of the system are preliminarily explored.

Robot error research is an important part of robot theory research[15-16]. The position and posture errors of a robot generally refer to the variation between the actual position and attitude of the end effector of the robot and the theoretical position and attitude. They are an important index for evaluating the motion quality of the robot. For Cable-typing close-coupling multi-robots towing system, most of the errors are caused by geometric errors of components, also known as original errors. The types of the original errors depend on the structure of the parallel robot, but there are mainly dimension errors, form errors, joint clearance errors, dynamic errors and so on. In addition, the parallel robot is also affected by system structure, assembly accuracy, transmission mechanism performance, process parameters and external environment. Therefore, it is necessary to carry out comprehensive error modeling and sensitivity analysis of parallel robots.

Aiming at the spatial position errors of the end effector of CCMRTS, the error constraint equation including error source is established by D-H method and matrix total differential method, and then the comprehensive error model is built. According to the model, the error analysis of parallel robot including pre-estimation of the accuracy, local sensitivity analysis, error source identification and motion reliability analysis are carried out. The instance simulation demonstrates the feasibility and effectiveness of the model and the algorithm.

2.Structural and Kinematic Analysis of CCMRTS

2.1Analysis of System Configuration

The structure diagram of CCMRTS is shown in Fig. 1.

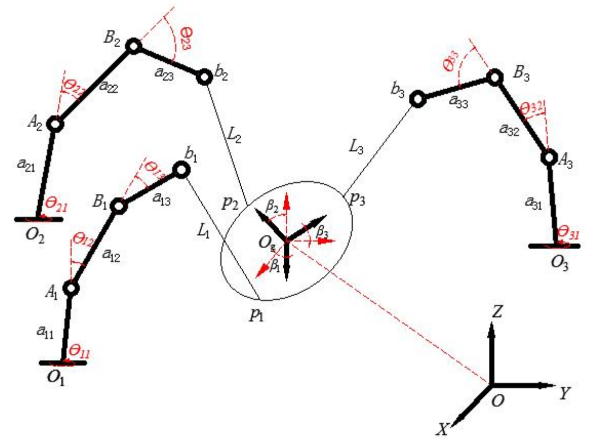

Fig. 1 Structure sketch of the CCMRTS

Three 3-DOF articulated manipulators which are fixed to the ground, parallel cable system and load together constitute the entire system. The load is connected to manipulator end-effectors by three cables and suspended below three manipulator end-effectors.

The global coordinate system O-XYZ and the local coordinate system O_i-$X_iY_iZ_i$ are established at the bottom of the robot. $\boldsymbol{P}_i$ is the connection point between the load and the cable, $\boldsymbol{b}$i is the connection point between the end of the robot and the cable, and $\boldsymbol{L}_i$ is the cable vector, where i=1,2,3 corresponds to three robots respectively. Establishment of load coordinate system O_g-XYZ at the center of mass of the load. (x,y,z)is the position vector of the transported object in the global coordinate system, $(\varphi_1, \varphi_2, \varphi_3)$ is the attitude angle of the transported object. a_{ij} is the length of the linkages of three robots and θ_{ij} is the joint angles of three robots.

2.2Kinematics Modeling of The System

Three cables can establish three equations of kinematics constrained. For the three robots in this paper coordinated lifting a load configuration, in order to ensure that the kinematics model is solved, assume that the three cables and the load intersect at the same point. Based on the spatial relationship, the position of the load in the workplace is determined by ：

$$\begin{cases} L_1^2 = (x - x_{b1})^2 + (y - y_{b1})^2 + (z - z_{b1})^2 \\ L_2^2 = (x - x_{b2})^2 + (y - y_{b2})^2 + (z - z_{b2})^2 \\ L_3^2 = (x - x_{b3})^2 + (y - y_{b3})^2 + (z - z_{b3})^2 \end{cases} \tag{1}$$

Fig. 2 is the schematic diagram of the local coordinates of the manipulator.

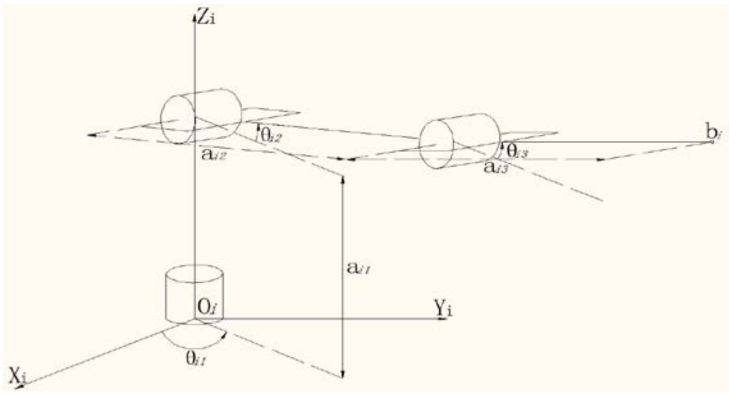

Fig. 2 Sketch of the manipulator

The joint angles of each arm are $(\theta_{i1}, \theta_{i2}, \theta_{i3})$. According to the method of D-H, the position of each manipulator end-effector in its local coordinate system is

$$\begin{cases} x_{bi}^* = c_{i1}c_{i2}c_{i3} - c_{i1}s_{i2}s_{i3} + c_{i1}c_{i2}a_{i2} \\ y_{bi}^* = s_{i1}c_{i2}c_{i3} - s_{i1}s_{i2}s_{i3} + s_{i1}c_{i2}a_{i2} \\ z_{bi}^* = a_{i1} - c_{i2}s_{i3}a_{i3} - c_{i3}s_{i2}a_{i3} - a_{i2}s_{i2} \end{cases} \tag{2}$$

where s_{i1}、s_{i2}、s_{i3} are the sine values of the three joint angles of the manipulator and c_{i1} 、c_{i2} 、c_{i3} are the cosine values of the three joint angles of the manipulator.

By the homogeneous coordinate transformation, the position of end-effectors in O-XYZ is given by

$$\begin{cases} x_{bi} = \cos(\alpha_i) x_{bi}^* - \sin(\alpha_i) y_{bi}^* + X_i \\ y_{bi} = \cos(\alpha_i) x_{bi}^* + \sin(\alpha_i) y_{bi}^* + Y_i \\ z_{bi} = z_{bi}^* \end{cases} \tag{3}$$

where α_i is a fixed value, which are Euler angles of the local coordinate system relative to inertial coordinate system. X_i、Y_i are fixed values which are the position of the origin of the local coordinate system in the inertial coordinate system.

3. The Model of Kinematic Error

3.1 Kinematic Error of Manipulators

Due to the influence of machining errors, assembling errors and abrasion, errors inevitably exist in the motion parameters and configuration parameters of the manipulator, resulting in errors in the position and pose of the output of the robot. Since the 3-DOF articulated manipulators used in this system are mainly used for terminal positioning, only the terminal position errors are calculated.

In practical application, the errors are minimal values relative to the size of the actual mechanism components. According to the error analysis theory, the corresponding errors are expressed by the differential forms of the relevant variables, and the total differential operation is carried out for Eq. (3):

$$\begin{cases} \mathrm{d}x_{bi} = \frac{\partial x_{bi}}{\partial a_{i1}}\mathrm{d}a_{i1} + \frac{\partial x_{bi}}{\partial a_{i2}}\mathrm{d}a_{i2} + \frac{\partial x_{bi}}{\partial a_{i3}}\mathrm{d}a_{i3} + \frac{\partial x_{bi}}{\partial \theta_{i1}}\mathrm{d}\theta_{i1} + \frac{\partial x_{bi}}{\partial \theta_{i2}}\mathrm{d}\theta_{i2} + \frac{\partial x_{bi}}{\partial \theta_{i3}}\mathrm{d}\theta_{i3} \\ \mathrm{d}y_{bi} = \frac{\partial y_{bi}}{\partial a_{i1}}\mathrm{d}a_{i1} + \frac{\partial y_{bi}}{\partial a_{i2}}\mathrm{d}a_{i2} + \frac{\partial y_{bi}}{\partial a_{i3}}\mathrm{d}a_{i3} + \frac{\partial y_{bi}}{\partial \theta_{i1}}\mathrm{d}\theta_{i1} + \frac{\partial y_{bi}}{\partial \theta_{i2}}\mathrm{d}\theta_{i2} + \frac{\partial y_{bi}}{\partial \theta_{i3}}\mathrm{d}\theta_{i3} \\ \mathrm{d}z_{bi} = \frac{\partial z_{bi}}{\partial a_{i1}}\mathrm{d}a_{i1} + \frac{\partial z_{bi}}{\partial a_{i2}}\mathrm{d}a_{i2} + \frac{\partial z_{bi}}{\partial a_{i3}}\mathrm{d}a_{i3} + \frac{\partial z_{bi}}{\partial \theta_{i1}}\mathrm{d}\theta_{i1} + \frac{\partial z_{bi}}{\partial \theta_{i2}}\mathrm{d}\theta_{i2} + \frac{\partial z_{bi}}{\partial \theta_{i3}}\mathrm{d}\theta_{i3} \end{cases} \tag{4}$$

Simplify the above formula into matrix form, and obtain the error model of manipulators as

$$\begin{bmatrix} \mathrm{d}\,x_{bi} \\ \mathrm{d}\,y_{bi} \\ \mathrm{d}\,z_{bi} \end{bmatrix} = \begin{bmatrix} \frac{\partial x_{bi}}{\partial a_{i1}} & \frac{\partial x_{bi}}{\partial a_{i2}} & \frac{\partial x_{bi}}{\partial a_{i3}} & \frac{\partial x_{bi}}{\partial \theta_{i1}} & \frac{\partial x_{bi}}{\partial \theta_{i2}} & \frac{\partial x_{bi}}{\partial \theta_{i3}} \\ \frac{\partial y_{bi}}{\partial a_{i1}} & \frac{\partial y_{bi}}{\partial a_{i2}} & \frac{\partial y_{bi}}{\partial a_{i3}} & \frac{\partial y_{bi}}{\partial \theta_{i1}} & \frac{\partial y_{bi}}{\partial \theta_{i2}} & \frac{\partial y_{bi}}{\partial \theta_{i3}} \\ \frac{\partial z_{bi}}{\partial a_{i1}} & \frac{\partial z_{bi}}{\partial a_{i2}} & \frac{\partial z_{bi}}{\partial a_{i3}} & \frac{\partial z_{bi}}{\partial \theta_{i1}} & \frac{\partial z_{bi}}{\partial \theta_{i2}} & \frac{\partial z_{bi}}{\partial \theta_{i3}} \end{bmatrix} \begin{bmatrix} \mathrm{d}\,a_{i1} \\ \mathrm{d}\,a_{i2} \\ \mathrm{d}\,a_{i3} \\ \mathrm{d}\,\theta_{i1} \\ \mathrm{d}\,\theta_{i2} \\ \mathrm{d}\,\theta_{i3} \end{bmatrix} \tag{5}$$

The upper form can be expressed as

$$\mathrm{d}\,\boldsymbol{e}_{bi} = \boldsymbol{J}_{bi}\,\mathrm{d}\,\boldsymbol{q}_{bi} \tag{6}$$

Where

$$\mathrm{d}\,\boldsymbol{e}_{bi} = [\mathrm{d}\,x_{bi}, \mathrm{d}\,y_{bi}, \mathrm{d}\,z_{bi}]^{\mathrm{T}} \tag{7}$$

$$\mathrm{d}\,\boldsymbol{q}_{bi} = [\mathrm{d}\,a_{i1,}\ \mathrm{d}\,a_{i2,}\ \mathrm{d}\,a_{i3,}\ \mathrm{d}\,\theta_{i1,}\ \mathrm{d}\,\theta_{i2,}\ \mathrm{d}\,\theta_{i3}]^{\mathrm{T}} \tag{8}$$

$\mathrm{d}\,\boldsymbol{e}_{bi}$ is the terminal error of each robot, $\mathrm{d}\,\boldsymbol{q}_{bi}$ is the parameter error caused by each error source, and $\boldsymbol{J}_{bi}$ is the error transfer matrix and non-singular matrix.

3.2 Error Model of Parallel Cable System

The position of the load in the workplace is determined by the equations of kinematics constrained in the workplace. Express equations as error sources as an independent variable:

$$f_i = (x, y, z, x_{b1}, y_{b1}, z_{b1}, x_{b2}, y_{b2}, z_{b2}, x_{b3}, y_{b3}, z_{b3}, L_1, L_2, L_3) = 0 \tag{9}$$

The total differential operation is carried out for Eq. (9):

$$\begin{aligned} \frac{\partial f_i}{\partial x}\mathrm{d}\,x + \frac{\partial f_i}{\partial y}\mathrm{d}\,y + \frac{\partial f_i}{\partial z}\mathrm{d}\,z = -\frac{\partial f_i}{\partial x_1}\mathrm{d}\,x_1 - \frac{\partial f_i}{\partial y_1}\mathrm{d}\,y_1 - \frac{\partial f_i}{\partial z_1}\mathrm{d}\,z_1 - \frac{\partial f_i}{\partial x_2}\mathrm{d}\,x_2 \\ -\frac{\partial f_i}{\partial y_2}\mathrm{d}\,y_2 - \frac{\partial f_i}{\partial z_2}\mathrm{d}\,z_2 - \frac{\partial f_i}{\partial x_3}\mathrm{d}\,x_3 - \frac{\partial f_i}{\partial y_3}\mathrm{d}\,y_3 \\ -\frac{\partial f_i}{\partial z_3}\mathrm{d}\,z_3 - \frac{\partial f_i}{\partial L_1}\mathrm{d}\,L_1 - \frac{\partial f_i}{\partial L_2}\mathrm{d}\,L_2 - \frac{\partial f_i}{\partial L_3}\mathrm{d}\,L_3 \end{aligned} \tag{10}$$

Simplify the above formula into matrix form:

$$\begin{bmatrix} \mathrm{d}x \\ \mathrm{d}y \\ \mathrm{d}z \end{bmatrix} = \begin{bmatrix} x-x_1 & y-y_1 & z-z_1 \\ x-x_2 & y-y_2 & z-z_2 \\ x-x_3 & y-y_3 & z-z_3 \end{bmatrix}^{-1} \begin{bmatrix} x-x_1 & 0 & 0 \\ y-y_1 & 0 & 0 \\ z-z_1 & 0 & 0 \\ 0 & x-x_2 & 0 \\ 0 & y-y_2 & 0 \\ 0 & z-z_2 & 0 \\ 0 & 0 & x-x_3 \\ 0 & 0 & y-y_3 \\ 0 & 0 & z-z_3 \\ L_1 & 0 & 0 \\ 0 & L_2 & 0 \\ 0 & 0 & L_3 \end{bmatrix}^{\mathrm{T}} \begin{bmatrix} \mathrm{d}x_1 \\ \mathrm{d}y_1 \\ \mathrm{d}z_1 \\ \mathrm{d}x_2 \\ \mathrm{d}y_2 \\ \mathrm{d}z_2 \\ \mathrm{d}x_3 \\ \mathrm{d}y_3 \\ \mathrm{d}z_3 \\ \mathrm{d}L_1 \\ \mathrm{d}L_2 \\ \mathrm{d}L_3 \end{bmatrix} \tag{11}$$

The upper form can be expressed as

$$\mathrm{d}\boldsymbol{e}_0 = \boldsymbol{J}_0\,\mathrm{d}\boldsymbol{q}_0 \tag{12}$$

where

$$\mathrm{d}\boldsymbol{e}_0 = [\mathrm{d}x, \mathrm{d}y, \mathrm{d}z]^{\mathrm{T}} \tag{13}$$

$$\mathrm{d}\boldsymbol{q}_0 = [\mathrm{d}x_1, \mathrm{d}y_1, \mathrm{d}z_1, \mathrm{d}x_2, \mathrm{d}y_2, \mathrm{d}z_2, \mathrm{d}x_3, \mathrm{d}y_3, \mathrm{d}z_3, \mathrm{d}L_1, \mathrm{d}L_2, \mathrm{d}L_3] \tag{14}$$

$\mathrm{d}\boldsymbol{e}_0$ position error of load, $\mathrm{d}\boldsymbol{q}_0$ stands for the end position errors of three robots and errors of parallel cable system, and $\boldsymbol{J}_0$ is the error transfer matrix and non-singular matrix.

It is concluded from Eq. (11) that position error of load is related not only to length error of cable but also to terminal errors of each robot.

3.3 Error Synthesis Model

Synthetic volumetric error model which contains all errors caused by error sources is built based on kinematics model of CCMRTS simultaneous kinematic error of manipulators and error model of parallel cable system. It is evaluated by

$$\mathrm{d}\boldsymbol{e} = \boldsymbol{J}_0 \begin{bmatrix} \begin{bmatrix} \boldsymbol{J}_{b1}\,\mathrm{d}\boldsymbol{q}_{b1} \\ \boldsymbol{J}_{b2}\,\mathrm{d}\boldsymbol{q}_{b2} \\ \boldsymbol{J}_{b3}\,\mathrm{d}\boldsymbol{q}_{b3} \end{bmatrix}^{\mathrm{T}}, \mathrm{d}L_1, \mathrm{d}L_2, \mathrm{d}L_3 \end{bmatrix}^{\mathrm{T}} \tag{15}$$

Eq. (15) can be expressed as

$$\mathrm{d}\boldsymbol{e} = \boldsymbol{J}\,\mathrm{d}\boldsymbol{q} \tag{16}$$

where

$$\mathrm{d}\boldsymbol{e} = [\mathrm{d}x, \mathrm{d}y, \mathrm{d}z]^{\mathrm{T}} \tag{17}$$

$$\mathrm{d}\boldsymbol{q} = [\mathrm{d}\boldsymbol{q}_{b1}{}^{\mathrm{T}}, \mathrm{d}\boldsymbol{q}_{b2}{}^{\mathrm{T}}, \mathrm{d}\boldsymbol{q}_{b3}{}^{\mathrm{T}}, \mathrm{d}L_1, \mathrm{d}L_2, \mathrm{d}L_3]^{\mathrm{T}} \tag{18}$$

Coupled $\boldsymbol{J}_{bi}$ and $\boldsymbol{J}_0$ to get $\boldsymbol{J}$. $\boldsymbol{J}$ is given by

$$\boldsymbol{J} = \begin{bmatrix} x-x_1 & y-y_1 & z-z_1 \\ x-x_2 & y-y_2 & z-z_2 \\ x-x_3 & y-y_3 & z-z_3 \end{bmatrix}^{-1} \begin{bmatrix} x-x_1 & 0 & 0 \\ y-y_1 & 0 & 0 \\ z-z_1 & 0 & 0 \\ 0 & x-x_2 & 0 \\ 0 & y-y_2 & 0 \\ 0 & z-z_2 & 0 \\ 0 & 0 & x-x_3 \\ 0 & 0 & y-y_3 \\ 0 & 0 & z-z_3 \\ L_1 & 0 & 0 \\ 0 & L_2 & 0 \\ 0 & 0 & L_3 \end{bmatrix}^{\mathrm{T}} \begin{bmatrix} \boldsymbol{J}_{b1} & & & & & 0 \\ & \boldsymbol{J}_{b2} & & & & \\ & & \boldsymbol{J}_{b3} & & & \\ & & & 1 & & \\ & & & & 1 & \\ 0 & & & & & 1 \end{bmatrix} \tag{20}$$

d$\boldsymbol{e}$ is position error of load, d$\boldsymbol{q}$ is error source which contains all sources from three robots and three cables, and $\boldsymbol{J}$ is the error transfer matrix of CCMRTS.

Replacing $d\boldsymbol{e}$ and $d\boldsymbol{q}$ with error forms $\Delta\boldsymbol{e}$ and $\Delta\boldsymbol{q}$,we can get the error compensation model:

$$\Delta\boldsymbol{e} = \boldsymbol{J}\Delta\boldsymbol{q} \tag{20}$$

4. Model Sensitivity Analysis

4.1 Precision Prediction of Errors

Taking a modular operation on the Eq. (20)

$$\begin{aligned} \|\Delta\boldsymbol{e}\|^2 &= \Delta\boldsymbol{e}^{\mathrm{T}}\Delta\boldsymbol{e} = \Delta\boldsymbol{q}^{\mathrm{T}}\boldsymbol{J}_{\Delta}{}^{\mathrm{T}}\boldsymbol{J}_{\Delta}\Delta\boldsymbol{q} \\ &= \sum_{i=1}^{21}\sum_{i=1}^{21}(\sum_{k=1}^{3} J_{\Delta ki}J_{\Delta ki})\Delta q_i\Delta q_i \end{aligned} \tag{21}$$

$J_{\Delta ki}$ represents the element in the k[th] row and the i[th] column of the matrix $\boldsymbol{J}$. Δq_i represents the element in the i[th] row of the errors vector $\Delta\boldsymbol{q}$.

Let the random parameters of the system are mutually independent and obey the normal distribution with the mean value of 0, we have $E(\Delta\boldsymbol{q}) = 0$, $E(\Delta\boldsymbol{e}) = 0$. Through the error mapping relationship we can get:

$$\mathrm{E}(\Delta\boldsymbol{e}^2) = \sum_{i=1}^{21}(\sum_{k=1}^{3} J_{\Delta ki}^2)\,\mathrm{E}(\Delta q_i{}^2) \tag{22}$$

Further, the variances of error sources and position errors of load satisfy

$$\mathrm{D}(\Delta \boldsymbol{e}) = \sum_{i=1}^{21} (\sum_{k=1}^{3} J_{\Delta ki}^{2}) \mathrm{D}(\Delta q_i) \tag{23}$$

Then from the first equation, we have standard deviation relationship between Δq and Δe is

$$\sigma(\Delta \boldsymbol{e}) = \sqrt{\sum_{i=1}^{21} (\sum_{k=1}^{3} J_{\Delta ki}^{2}) \sigma^2 (\Delta q_i^{\,2})} \tag{24}$$

It can be seen from the inference above that the accuracy of position errors of load can be predicted by the variance value of 21 error sources. Without losing its generality, when confidence coefficient is 3, confidence probability is 99.73%. According to 3σ principle, the precision prediction interval of load position error is $\left(-3\sigma(\Delta \boldsymbol{e}), 3\sigma(\Delta \boldsymbol{e})\right)$.

4.2. Local Error Sensitivity

According to the previous deduction, when the errors caused by error sources change slightly, the position error of the load will change correspondingly, which is defined as the error sensitivity. Therefore, the position error of the load to 21 error sources is

$$S_i = \sqrt{\sum_{k=1}^{3} J_{\Delta ki}^{2}} \qquad (i = 21) \tag{25}$$

As it is seen from the Eq. (25), the error sensitivity is not only related to the spatial configuration of the system, but also to the space position coordinates of the end-effector. The error sensitivity changes with the position workspace of the end-effector. So the aforementioned error sensitivity which only reflects error sensitivity of the system in the local design space is called local error sensitivity.

For measuring error sensitivity in the whole space，we define global average error sensitivity which is the average of local error sensitivity in whole design space. It is evaluated by

$$\overline{S_i} = (\int_V S_i dV) / V \qquad (i = 21) \tag{26}$$

Reduce the value of the global average error sensitivity and deal with dimensionless. We can get that the error sensitivity coefficient corresponding to the errors caused by error sources Δq is

$$K_i = \overline{S_i} / \sum_{i=1}^{21} \overline{S_i} \tag{27}$$

Eq.(27) is the model of CCMRTS under statistical significance and satisfies $\sum_{i=1}^{21} K_i = 1$. It can identify, analyze and compare critical error sources better[1].

5 Kinematic Reliability Analysis of CCMRTS

5.1 Kinematic Reliability Model

The whole mechanical arm parameters and rope length parameters are all distributed normally, that is $\boldsymbol{q}$~(μ_x, σ^2_x). Now according to synthetic volumetric error model analysis kinematic reliability of load.

The motion error is the difference between the actual motion output $\boldsymbol{p}$ and the desired motion output $\boldsymbol{p}_d$ in all motion cycle. It is given by

$$\mathrm{g}(\boldsymbol{q},t) = \boldsymbol{p} - \boldsymbol{p}_d \tag{28}$$

According to Eq. (20) , Eq. (28)can be expressed as

$$\mathrm{g}(\boldsymbol{q},t) = \Delta\boldsymbol{p} = \boldsymbol{J}\Delta\boldsymbol{q} \tag{29}$$

To ensure that the mechanism work properly, the motion error must be less than the allowable error $\boldsymbol{\varepsilon}$, that is

$$\left|g(\boldsymbol{q},t)\right| \le \boldsymbol{\varepsilon} \tag{30}$$

That is to say, the position errors of the transported object in each direction should not exceed the maximum allowable value.

The reliability is measured by the probability that the desired function is realized within the specified error $\boldsymbol{\varepsilon}$. It is evaluated by

$$\boldsymbol{R}(t) = \Pr\left\{\left|\mathrm{g}(\boldsymbol{q},t)\right| \le \boldsymbol{\varepsilon}\right\} \tag{31}$$

The failure probability is

$$\boldsymbol{p}(t) = \Pr\left\{\left|\mathrm{g}(\boldsymbol{q},t)\right| \succ \boldsymbol{\varepsilon}\right\} \tag{32}$$

The kinematic reliability of load in the three directions of X, Y, and Z in the global coordinate system can be expressed as $\boldsymbol{R}(t) = (R_x(t), R_y(t), R_z(t))$.

5.2 Solution of Kinematic Reliability

The reliability can be calculated by the first-order second moment (FOSM) method

$$R = 2\Phi\left(\frac{\varepsilon - \mu_g(X)}{\sigma_g(X)}\right) - 1 \tag{33}$$

The standard deviation of system output error can be determined by Eq.(22). The motion variables and input parameters of the whole system obey the normal distribution of the mean value of 0, and the motion output error of the robot obeys the normal distribution of the mean value of 0. It means $\mu_g(X) = 0$. ε is the allowable error range of the system.

6. Numerical Simulation and Analysis

The numerical simulation of error synthesis model, sensitivity model and kinematic reliability model are carried out by using MATLAB. Programming and drawing with MATLAB.

The configuration parameters of three 3-DOF robots are

$$\begin{cases} \boldsymbol{a}_{i1} = 300\,\text{mm} \\ \boldsymbol{a}_{i2} = 410\,\text{mm} \qquad (\boldsymbol{i} = 1,2,3) \\ \boldsymbol{a}_{i3} = 500\,\text{mm} \end{cases} \tag{34}$$

The length of the three cables is $L_1 = L_2 = L_3 = 800\,\text{mm}$. The initial coordinates of the three robot bases in the global coordinate system are $(0,0,0)$, $(432\,\text{mm}, 750\,\text{mm}, 0)$, $(860\,\text{mm}, 0, 0)$. Fig.3 is the sketch of the mechanism set up during the simulation.

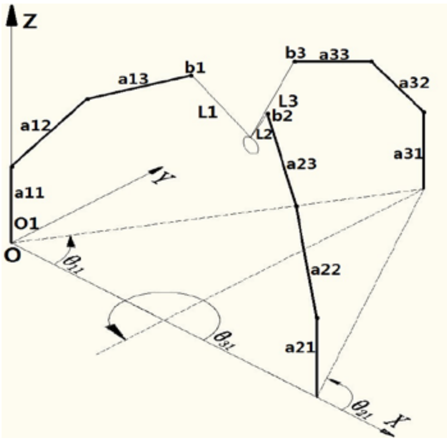

Fig. 3 Structure sketch of the simulation

The motion laws of the three robots are as follows:

$$\begin{cases} \theta_{11} = \dfrac{\pi}{6} + \dfrac{1}{4}\sin(0.5\boldsymbol{t}) \\ \theta_{12} = \dfrac{\pi}{12} + \dfrac{1}{6}\sin(0.5\boldsymbol{t}) \\ \theta_{13} = \dfrac{\pi}{3} + \dfrac{1}{8}\sin(0.5\boldsymbol{t}) \end{cases} \tag{35}$$

$$\begin{cases} \theta_{21} = \frac{5\pi}{6} + \frac{1}{4}\sin(0.5\boldsymbol{t}) \\ \theta_{22} = \frac{\pi}{12} + \frac{1}{6}\sin(0.5\boldsymbol{t}) \\ \theta_{23} = \frac{\pi}{3} + \frac{1}{8}\sin(0.5\boldsymbol{t}) \end{cases} \tag{36}$$

$$\begin{cases} \theta_{31} = \frac{3\pi}{2} + \frac{1}{4}\sin(0.5\boldsymbol{t}) \\ \theta_{32} = \frac{\pi}{12} + \frac{1}{6}\sin(0.5\boldsymbol{t}) \\ \theta_{33} = \frac{\pi}{3} + \frac{1}{8}\sin(0.5\boldsymbol{t}) \end{cases} \tag{37}$$

Set the variance value of the 21 errors caused by sources errors of CCMRTS which obey the normal distribution and have a mean of 0.

Table1

The variance of 21 errors caused by error sources in the system

D(Δq)	Δa_{i1}(mm)	Δa_{i2}(mm)	Δa_{i3}(mm)	$\Delta\theta_{i1}$(rad)	$\Delta\theta_{i2}$(rad)	$\Delta\theta_{i3}$(rad)	ΔL_i(mm)
i=1	0.0301	0.0471	0.0230	0.0044	0.0095	0.0026	0.0171
i=2	0.0301	0.0471	0.0230	0.0044	0.0095	0.0026	0.0171
i=3	0.0301	0.0471	0.0230	0.0044	0.0095	0.0026	0.0171

6.1 Trajectory and Motion Errors

The trajectory of the object is a smooth curve. Fig. 4 shows the motion errors of loads in X, Y and Z directions during the motion cycle.

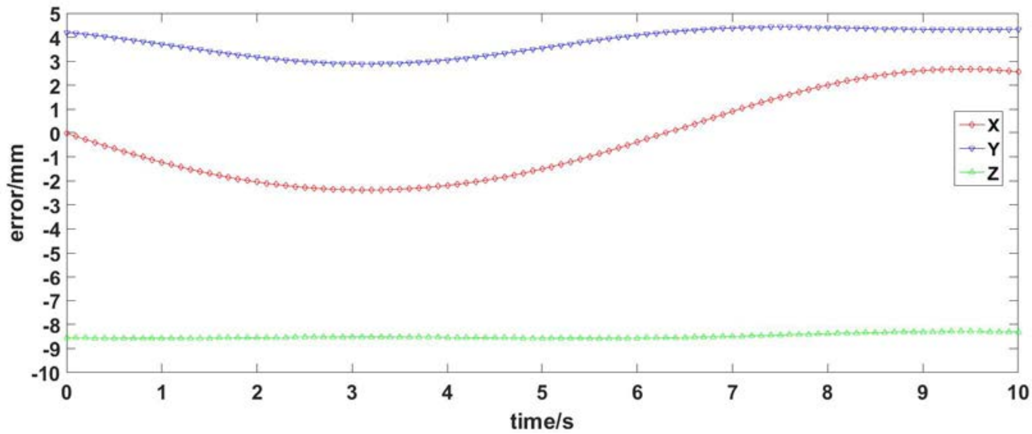

Fig. 4 the motion errors of loads in X, Y and Z directions

Compared the three curves in Fig. 4, we can see that the errors of the lifts in the three directions of X, Y and Z change with time, but they are within the error limits.

6.2 Error Sensitivity

Fig. 5 to Fig. 11 show the local error sensitivity curves of 21 error sources.

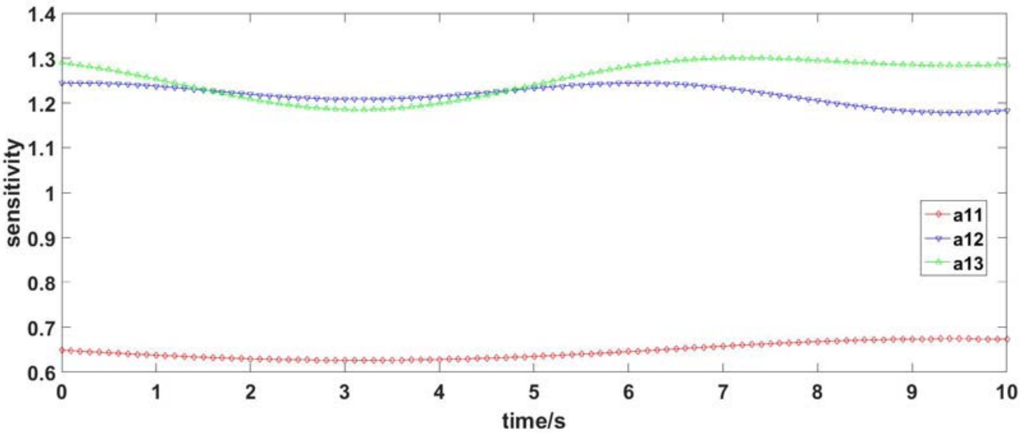

Fig. 5 the local sensitivity of *a11*,*a12*,*a13*

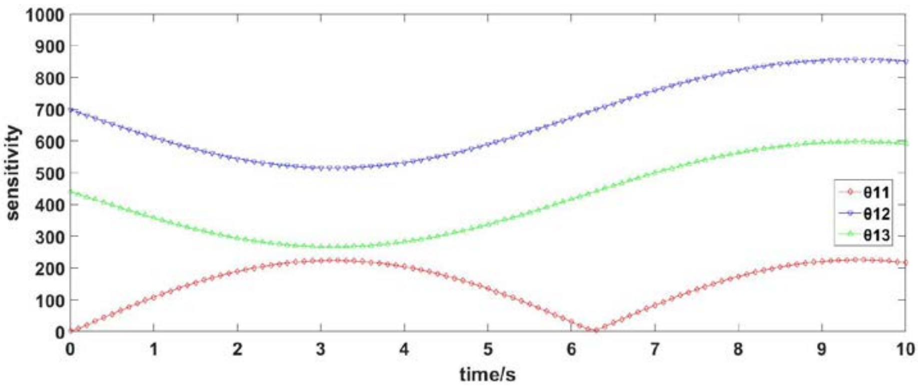

Fig. 6 the local sensitivity of $\theta_{11}, \theta_{12}, \theta_{13}$

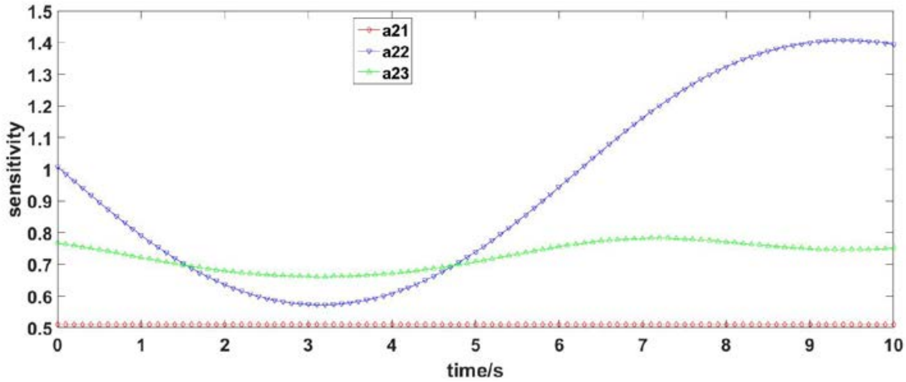

Fig. 7 the local sensitivity of a_{11},a_{12},a_{13}

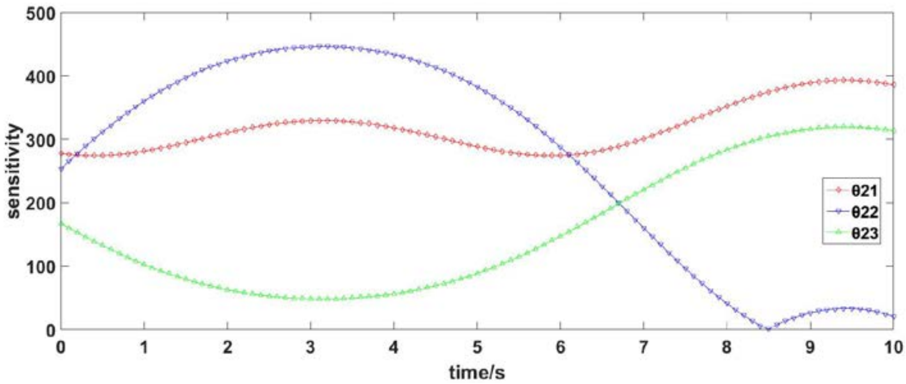

Fig. 8 the local sensitivity of $\theta_{21},\theta_{22},\theta_{23}$

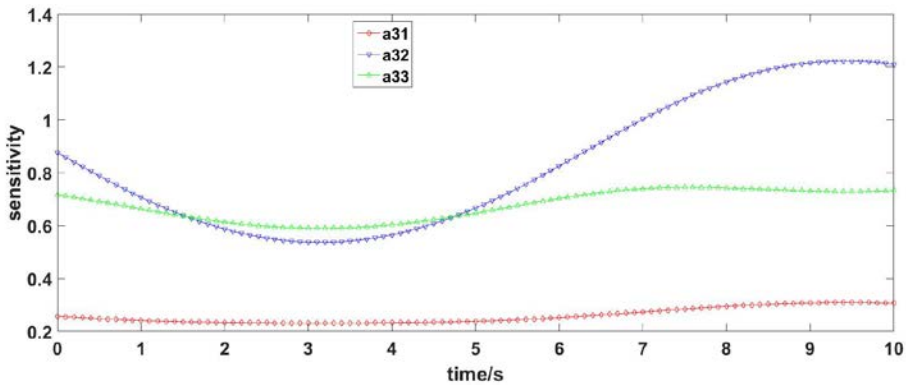

Fig. 9 the local sensitivity of a_{31},a_{32},a_{33}

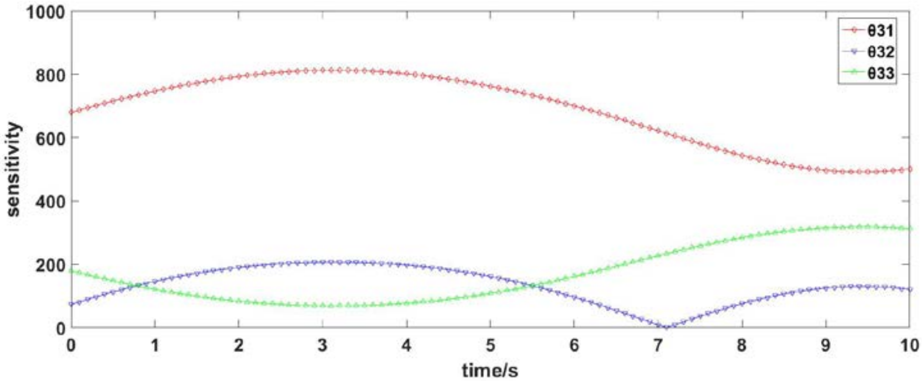

Fig. 10 the local sensitivity of $\theta_{31}, \theta_{32}, \theta_{33}$

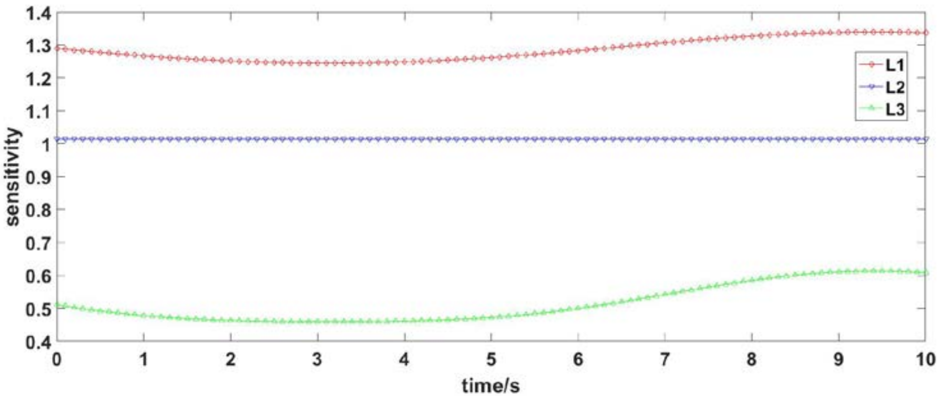

Fig. 11 the local sensitivity of *L1,L2,L3*

Compared with Fig. 5 to Fig. 10, the local sensitivity of nine joint angles of three robots in the 21 error sources of the whole system is larger and the range of variation is larger than that of other error sources. Therefore, errors of the manipulator joint motion have the greatest impact on position errors of load in the whole system, followed by errors of rod length of manipulators and cable respectively.

Compared with Fig. 5 to Fig. 11 and the input parameters of kinematics of the system, although the structural parameters of the three robots are identical, the motion rules of the whole motion cycle are identical, and the input of the rope length is identical, the variation range and rule of the local error sensitivity of each parameter are very different. The nonlinearity and complexity of the system are fully explained, and the generality and validity of the model are also verified.

6.3 Kinematic Reliability Analysis

The failure probability of load in X, Y and Z directions can be obtained by solving the reliability model of robot motion accuracy with Eq. (33). If the position errors of the load are too large, that is, the differences between the desired motion outputs and the actual motion outputs are too large, the system is considered to be invalid. In order to ensure the effectiveness of the system, the position errors of the load are limited to a range. According to the structural parameters and kinematic parameters of the system set in this paper It is assumed that the allowable range of errors in all three directions is $\pm 10mm$.

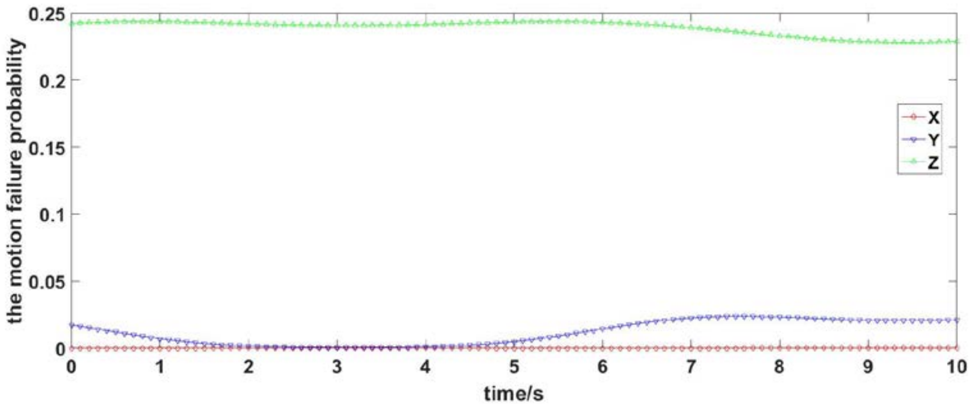

Fig. 12 the motion failure probability of loads in X, Y and Z directions

From Fig. 12, the reliability varies with time in the whole motion cycle and working space, indicating that the structural parameters and motion parameters of the system have different effects on its motion accuracy at different time points. Comparing the failure probability of the object being lifted in the X, Y, and Z directions, the probability of failure in the Z direction is the largest. From this, it can be seen that CCMRTS has a lower motion accuracy in the Z direction than in the X and Y directions under the aforementioned motion parameters.

7. Conclusions

In this paper, the comprehensive error analysis of CCMRTS is carried out. Through calculation and simulation, the following innovative works and conclusions are completed for CCMRTS:

(1) Based on the kinematics model of the multi-machine combined lifting system, the comprehensive error model of the system is established by using the

total differential method. This paper effectively integrates the error model of manipulators and parallel cable system. The position errors of load in three directions are compared by numerical simulation.

(2) The error sensitivity analysis is completed. The error sensitivity model of the system is established. The influence of 21 error sources on the output parameters of the system is compared quantitatively. The complexity and nonlinearity of the system are verified. It also provides a theoretical basis for the design of mechanism configuration.

(3) Reliability analysis completed. The reliability model of the system's motion accuracy is established and solved by the first-order second-moment method. The reliability of the movement accuracy of the lifted object in different directions is compared. Analyzes the probabilities of system failure due to errors during the work process.

In this paper, two kinds of error sources affecting the position error of load space are refined into 21 error sources, and the error studies mainly focus on the precision prediction of errors, local sensitivity analysis and reliability analysis are carried out. However, this paper only considers the position error of the load. In the future, the position error and attitude error of the load should be synthesized to carry out the trajectory planning of CCMRTS under uncertainty.

Acknowledgments

This project is supported by National Natural Science Foundation of China (Grant No.51265021,11462011).

R E F E R E N C E S

[1]. *B. Zi*, Mechanics analysis and tracking control technology of hybrid-driven based cable parallel robots,Beijing: Science Press, 2013

[2]. *N. Michael, J. Fink, V. Kumar*,“Cooperative manipulation and transportation with aerial robots”, in Autonomous Robots., **vol. 30**, no. 1, 2011, pp. 73-86.

[3]. *Q. M. Jiang, V. Kumar*,“The inverse kinematics of cooperative muitiple aerial robots”, in IEEE Transportations On Robotics.,**vol. 29**, no. 1, 2013, pp. 135-145.

[4]. *J. Fink, N. Michael, V. Kumar, et al*,“Planning and control for cooperative manipulation and transportation with aerial robots”, in The International Journal of Robotics Research.,**vol. 30**, no. 3, 2011, pp. 324-334.

[5]. *P. Cheng, J. Fink, S. Kim, et al*,“Cooperative Towing with Multiple Robots”, in Advanced Robotics.,**vol. 1**, no. 1, 2009, pp. 101-116.

[6]. *Y. Q. Zheng, Q. L, J. P Wu, et al*,“Analysis of inverse kinematics and dynamics of a novel 6-degree-of-freedom wire-driven parallel gantry crane robot”, in IEEE/ASME International Conference on Advanced Intelligent Mechatronics., Sept. 2009, pp. 1789-1791.

[7]. *L. Yu, Y. Q. Zheng*,“Configuration design and analysis of generalized inverse pose kinematic problem of 6-DOF wire-driven gantry crane robots”, in International Conference on Automatic Control and Artificial Intelligence .,**vol. 29**, no. 1, April,2013, pp. 676-680.

[8]. *B. Zi, Z. Q. Yin, Y. C. Li, et al*,“Fast mobile component location method for cable-driven parallel robots based on YOLO Model”, in Journal of Mechanical Engineering,**vol. 55**, no.4, 2019, pp.64-72.
[9]. *B. Zi, S. Qian, B. Zhou*,“Dynamic modeling and analysis of cable parallel manipulator for dual automobile cranes during luffing motion”, in Journal of Mechanical Engineering, **vol. 53**, no.7, 2017, pp.55-61.
[10]. *W. Li, Z. G. Zhao, G. T. Shi, et al*,“Solutions of kinematics and dynamics for parallel cable-driven system with multi-robots”, in Journal of Zhejiang University(Engineering Science), **vol. 49**, no.10, 2015, pp.1916-1923.
[11]. *Z. G. Zhao, T. S. Lu*,“Simulation on Kinematics and Stability of Multi-helicopters Hoist System”, in Journal of System Simulation, **vol. 4**, 2013, pp.790-794.
[12]. *Z. G. Zhao, Y. L. Wang, J. S. Li*,“Appraise of dynamical stability of multi-robots cooperatively towing system based on hybrid force-position-pose approach”, in Journal of Harbin Engineering University, **vol. 39**, no.1, 2018, pp.148-155.
[13]. *Z. G. Zhao, T. S. Lu*,“Coordinated Dynamic Load Distribution for Multi-robot Collaborative Towing System”, in Robot, **vol. 34**, no. 1, 2012, pp.114-119.
[14]. *Y. L. Wang, Z. G. Zhao,J.S. Li, et al*,“Analysis of Workspace of Cable-Typing Close-Coupling Multi-Robot Collaboratively Towing System”, in UPB Scientific Bulletin, Series D: Mechanical Engineering, **vol. 78**, no.4, 2016, pp.3-20.
[15]. *P. Majda*,“Modeling of geometric errors of linear guideway and their influence on joint kinematic error in machine tools”, in Precision Engineering, **vol. 36**, no.3, 2012, pp. 369-378.
[16]. *H. L. Shi, H. J. Su, N. Dagalakis, et al*,“Kinematic modeling and calibration of a flexure based hexapod nanopositioner”, in Precision Engineering, **vol. 37**, no. 1, 2013, pp. 117-128.